IOP Publishing Journal of Physics: Condensed Matter

J. Phys.: Condens. Matter **21** (2009) 496001 (6pp) doi:10.1088/0953-8984/21/49/496001

Time-resolved magnetization dynamics of cross-tie domain walls in permalloy microstructures

J Miguel[1], J Sánchez-Barriga[2], D Bayer[3], J Kurde[1], B Heitkamp[2], M Piantek[1], F Kronast[2], M Aeschlimann[3], H A Dürr[2] and W Kuch[1]

[1] Institut für Experimentalphysik, Freie Universität Berlin, Arnimallee 14, D-14195 Berlin, Germany

[2] Helmholtz-Zentrum Berlin für Materialien und Energie, Elektronenspeicherring BESSY II, Albert-Einstein-Straße 15, D-12489 Berlin, Germany

[3] Fachbereich Physik, Universität Kaiserslautern, Erwin-Schrödinger Straße 46, D-67663 Kaiserslautern, Germany

E-mail: jorge.miguel@fu-berlin.de

Received 28 August 2009, in final form 1 October 2009
Published 12 November 2009
Online at stacks.iop.org/JPhysCM/21/496001

Abstract

We report on a picosecond time-resolved x-ray magnetic circular dichroic-photoelectron emission microscopy study of the evolution of the magnetization components of a microstructured permalloy platelet comprising three cross-tie domain walls. A laser-excited photoswitch has been used to apply a triangular 80 Oe, 160 ps magnetic pulse. Micromagnetic calculations agree well with the experimental results, both in time and frequency, illustrating the large angle precession in the magnetic domains with magnetization perpendicular to the applied pulse, and showing how the magnetic vortices revert their core magnetization while the antivortices remain unaffected.

(Some figures in this article are in colour only in the electronic version)

1. Introduction

A deep understanding of the fundamental processes that govern the magnetization dynamics on the picosecond timescale is crucial to improve the efficiency and reliability of current and near-future information storage media. On such short timescales, precession of the atomic spins, rather than domain wall motion, dictates the response of quasi-two-dimensional magnetic structures [1, 2]. When finite-sized, soft magnetic microstructures are considered, the demagnetization energy forces the formation of flux-closure magnetic domain patterns that may contain domain walls (DWs) and circular or cross Bloch lines, also known as vortices or antivortices. These magnetic structures react at different times to fast magnetic pulses, resulting in a complex global behavior. In the simplest case, the response of a permalloy squared structure to a fast magnetic pulse comprises precession in the domains, oscillation of the domain walls and changes in the vortex positions. The latter may generate spin waves that interact with those originated at the domains [3–5]. Furthermore, due to its potential application on magnetic storage media, vortex core switching, a process in which the out-of-plane component of the magnetization is reversed while retaining the overall in-plane pattern, has lately blossomed in experimental [6, 7] and theoretical investigations [8–12].

Here we present a study comprising all the aforementioned aspects by comparing temporally resolved microscopy results of a permalloy (Py) rectangular microstructure with micromagnetic calculations based on the Landau–Lifshitz–Gilbert equation. The magnetic responses include the magnetization precession of the domains with magnetization oriented perpendicular to the field pulse direction, as well as the oscillation in domain walls, vortices, and antivortices. From the micromagnetic calculations we conclude that the vortices show much larger motions as compared to the ones of the antivortices, and that in certain cases the perpendicular component of the vortex magnetization can be switched at the applied pulse strength.

2. Experiment

We make use of the magnetic and element sensitivity of x-ray magnetic circular dichroism combined with the lateral

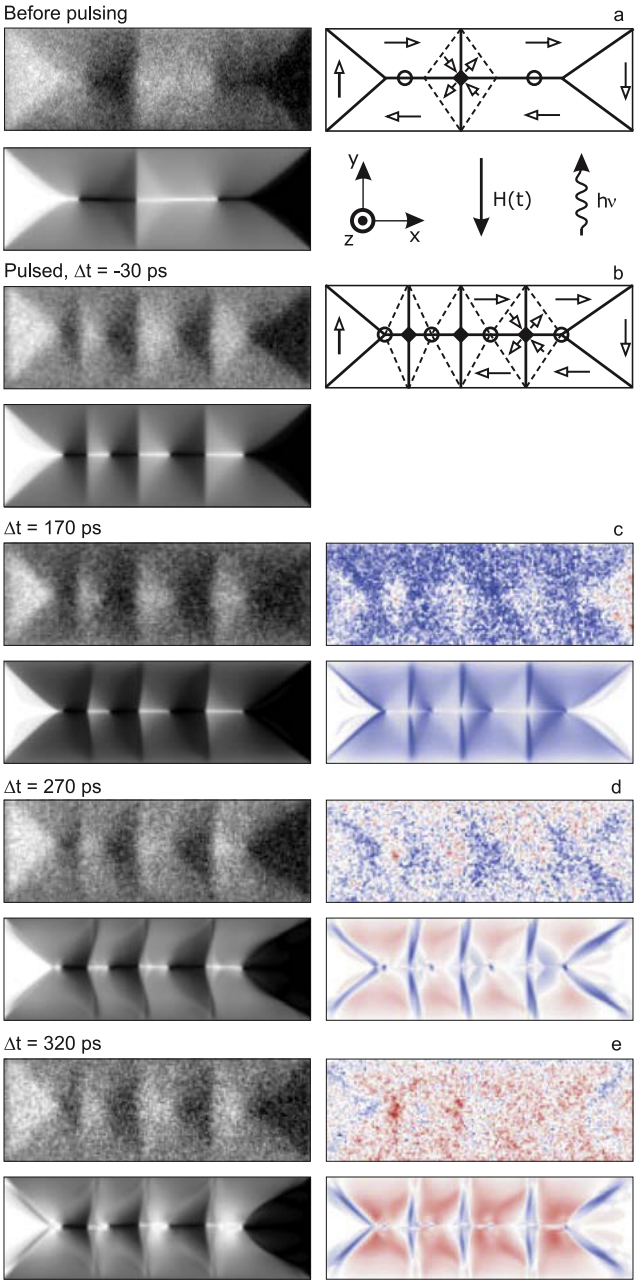

Figure 1. (a) Magnetic domain pattern of the as-grown state of the $5 \times 15\ \mu m^2$ Py microstructure as seen by XMCD-PEEM (top) and simulated by micromagnetic calculations (bottom). From (b)–(e), on the left, experimental (top) and calculated (bottom) images of the magnetic state after pulsing, at selected delay times. Difference images for the experimental and calculated results, using the $\Delta t = -30$ ps images as reference, are shown beside the corresponding images. Red (blue) indicates positive (negative) changes in the XMCD contrast, with white as neutral color. Schematic sketches of the magnetic domain patterns are shown for the as-grown (a) and pulsed (b) states, comprising 90° DWs (full lines), 45° DWs (dashed lines), vortices (○) and antivortices (◇). The relative directions of the magnetic field pulse and of the incoming x-rays are also shown.

resolution of photoelectron emission microscopy (XMCD-PEEM). Access to the temporal resolution is achieved by synchronizing a picosecond magnetic field excitation with an x-ray pulse that images the system. A stroboscopic pump–probe scheme was used in the measurements. By tuning the time delay between the arrivals of pump and probe, the time evolution of the system is followed. A femtosecond laser, operating at 800 nm wavelength and 62.5 MHz repetition frequency, excites electron–hole pairs in a photoconductive switch, subject to a constant voltage. The resulting pulsed current travels along a 10 μm wide Au stripline, creating a magnetic field pulse in the vicinity of the stripline surface that is measured by normalizing the distortion of the stripline PEEM image to the total current [13]. We achieved triangular pulses with rising and decaying slopes of about 80 ps (after deconvoluting the x-ray pulse length of 70 ps), and 80 Oe at the peak magnetic field, for 400 mW laser power, 80 V and 850 μA across the stripline (see figure 2(a)). The magnetization state of the microstructure is probed by the synchrotron x-ray pulses of BESSY II in the single-bunch mode (repetition rate of 1.25 MHz), so that the temporal resolution is ultimately limited by the ∼70 ps maximum x-ray pulse length. The evolution of the laterally resolved magnetization in the microstructure was followed by setting a delay time Δt between the laser pulse and the x-ray probe in steps of 50 ps, with $\Delta t = 0$ defined as the onset of the magnetic field pulse. The XMCD-PEEM images with magnetic sensitivity were calculated as the asymmetry of the images for left- and right-circularly polarized light. The 16 ns time interval between magnetic field pulses is more than sufficient for the microstructure magnetization to return to its initial configuration between pulses, as will be shown later.

A Focus IS-PEEM instrument at a lateral resolution of 500 nm [14], and a custom-made sample holder [15] were employed. A $5 \times 15\ \mu m^2$, 21.5 nm thick Py microstructure was deposited by magnetron sputtering onto the Au stripline. Electron-beam lithography was employed to define both the stripline and the magnetic microstructure. XMCD-PEEM images for different delay times are corrected for shifts and size changes that result from the distortion of the emitted electron trajectories during the pulse. In order to enhance the changes in the magnetic contrast, we calculated the differences of each image at the corresponding delay time relative to the image before the magnetic pulse at time $\Delta t = -30$ ps.

The micromagnetic calculations have been performed with the OOMMF software package [16], which solves the Landau–Lifshiftz–Gilbert equation [17] to relax three-dimensional spins in a two-dimensional squared mesh of half of the structure size. A $5 \times 5 \times 20\ nm^3$ cell size and the usual magnetic parameters for Py were input in the calculation: saturation magnetization $M_s = 796\ kA\,m^{-1}$, exchange constant $A = 1.3 \times 10^{-11}\ J\,m^{-3}$, magnetic damping constant $\alpha = 0.01$, and uniaxial anisotropy $K_u = 0$. The simulations were run until the total magnetic torque was smaller than 10^{-6} N m.

3. Results and discussion

Figure 1(a) shows the XMCD-PEEM image of the magnetic domain pattern in the as-grown state, sketched in the top right side of panel (a). It is formed by two flux-closing domain configurations in the periphery of the structure dressing two

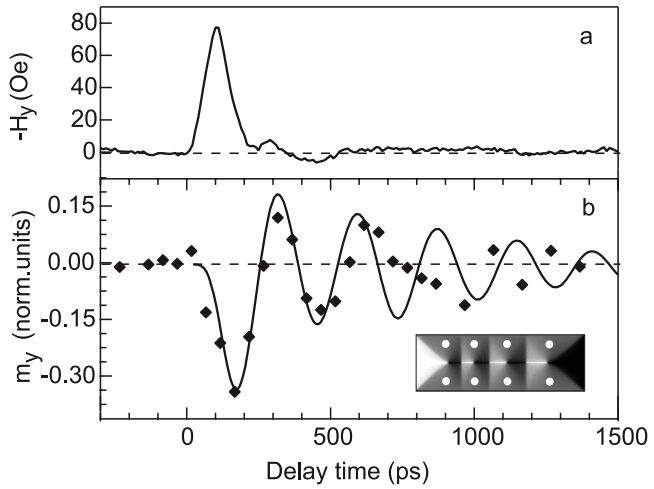

Figure 2. (a) Applied magnetic field pulse before deconvoluting with the x-ray pulse length. (b) Time-dependent XMCD contrast of the gray domains from the experimental data (symbols) and the OOMMF calculation (line). The inset marks the areas used for the integration.

vortices, whereas a cross-tie domain wall appears at the central part. This diamond-shaped magnetic structure comprises two 90° DWs crossing each other, four 45° DWs connecting their ends, and an antivortex in the crossing point. It serves to reduce the total magnetic energy compared, e.g. to a single 180° Néel wall across the two most distant vortices [18]. The asymmetric position of the vertical wall is most likely due to small defects that act as pinning centers, possibly at the structure boundaries. These defects were not included in the simulation, instead the positions of the vertical domain wall and vortices were used to draw a simplified domain pattern, whose $m_{x,y}$ magnetization distributions were set as the initial state in the calculations. The result of relaxing this domain pattern in the calculation is shown on the bottom left side of figure 1(a), yielding a good agreement with the experimental one. After applying magnetic field pulses the microstructure reached a magnetically lower energy state by irreversibly converting into a new domain pattern (top left in panel (b)), now displaying two additional cross-tie walls [19]. Further pulsing had no influence on the cross-tie configuration for several days of measurements, proving that it is one of the stable states.

In order to simulate the transition from the as-grown state to the pulsed domain state in the micromagnetic calculations, an external magnetic field pulse of triangular shape and 80 ps rising and decaying slopes was applied to the initially calculated single cross-tie wall state. Single pulses were able to create either one or two additional cross-tie walls. We can thus deduce that the effect of many more pulses used in the experiment saturates the magnetic structure with three cross-tie walls, the maximum number allowed by the lateral dimensions [20]. The slightly different positions of the two new vertical DWs as compared to the measured pattern can be assigned to local pinning centers. The deviation does not play an important role in the magnetization dynamics of the structure. We show in panels (c)–(e) measured images for selected delay times (top left), the corresponding calculated images (bottom left), and the respective difference images (right side). The most pronounced effect in the magnetic contrast appears 170 ps after the onset of the magnetic field pulse. This is when the magnetization in the magnetic domains that are initially magnetized along the x direction displays a maximum brightness reduction when compared to the reference image (displayed in blue in the difference image). These domains will be referred to as gray domains in the following. Such a behavior is expected, since the magnetization **m** of these domains is perpendicular to the applied magnetic pulse **H**, thus maximizing the magnetic torque $\boldsymbol{\tau} = \mathbf{m} \times \mathbf{H}$ caused by the field pulse. Although the resulting torque points along z, the demagnetization field allows only a small excursion into that direction. Analysis of the contrast yields a deviation angle of m_y from the static orientation of about 20°. At larger delay times, the XMCD contrast in the gray domains vanishes and reverses its sign, following a damped quasi-harmonic oscillation with a frequency around 3.3 GHz. This can be clearly seen in the time dependence of the integrated XMCD contrast of small areas in the gray domains (figure 2). There is a good agreement between the XMCD contrast of the central gray domains and the corresponding curve obtained from the calculated images. These changes in magnetic contrast can be addressed to an attenuated quasi-harmonic magnetization precession in the gray domains, at least during the first and second periods.

Another important magnetic effect appears at the 90° DWs dressing the black and white domains and at those of the cross-tie walls. In order to illustrate this, we show in figure 1(d) the images for $\Delta t = 270$ ps. Compared to the magnetization precession in the gray domains, these DWs have a longer oscillation period, as indicated by the blue and red areas in the difference images. Although the magnetic torque in the black and white domains is zero, both are affected by the large oscillation of their DWs [5]. At $\Delta t = 320$ ps, the deviation of m_y in the gray domains has completely reversed with respect to the situation at $\Delta t = 170$ ps. The initial magnetic domain structure is recovered after 1.5 ns (data not shown).

Deeper insight into the magnetization dynamics of the structure can be gained by computing the Fourier transform of the measured and calculated images, yielding a laterally resolved image of the most important frequencies present in this microstructure. The 800 ps time interval taken with a constant time step yields a FT frequency step of 1.25 GHz. A 2×2 binning was applied to the XMCD-PEEM images, improving the signal-to-noise level. The resulting amplitudes and phases of the Fourier-transformed images are shown in figure 3. Merely two frequencies show high amplitudes, around 1.25 GHz (a) and 3.75 GHz (b), finding a reasonable agreement between experiment and simulation. At 1.25 GHz only the diagonal and vertical 90° DWs are affected, although the vortices and antivortices also display some amplitude. In contrast, the gray domains are active at 3.75 GHz, in agreement with the frequency found in figure 2. Panel (c) shows the Fourier spectra obtained from m_y of the full simulated structure, and from areas located at the gray domains and at the DWs of the measured images. We observe that the main frequencies at the domains and DWs coincide with the simulated ones, although contributions from other components

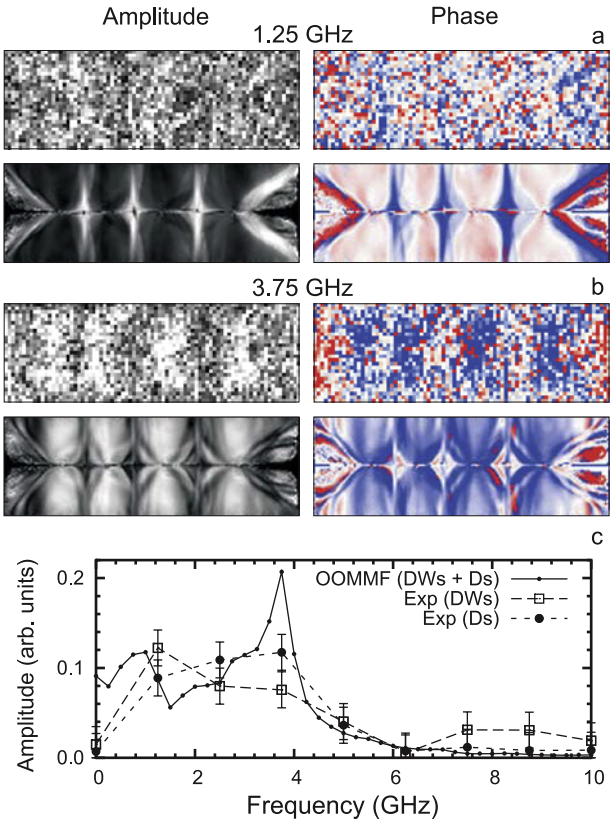

Figure 3. Laterally resolved images of the amplitude (left) and phase (right) for (a) 1.25 GHz and (b) 3.75 GHz, obtained from the Fourier transform of the time-dependent experimental results (top) and calculations (bottom). On the right side, +90° (−90°) phase is indicated in red (blue). (c) Fourier analysis of the full simulated structure (full line), and of experimental areas on the gray domains (●) and domain walls (□).

are not negligible. These results agree qualitatively with previous studies in similar systems [21, 22]. Discrepancies in the observed frequencies can be due to the different pulse shapes used in those experiments.

It has been observed that the signs of the m_z components of the vortex and antivortex cores play an important role for the magnetization dynamics in a single cross-tie wall [23], resulting in different amplitudes of the core gyration upon their relative orientations. We show in figure 4 calculated color-coded plots of m_z in areas near several vortex and antivortex cores at some selected delay times during the first half of the oscillation period of the gray domains, where red (blue) indicates positive (negative) magnetization. Completely different behaviors are apparent for an antivortex (a) and a vortex (b), both pointing up. While the antivortex core remains relatively unaffected by the magnetic pulse, the vortex core is strongly perturbed. Firstly, a core with opposite m_z appears next to the pre-existing one as in a magnetic dipole, approximately when the precession in the gray domains reaches its maximum ($\Delta t = 150$ ps). These two cores collapse onto each other in an annihilation process, creating a series of circular spin waves that travel away from the initial core position. At $\Delta t = 281$ ps a clear vortex core is visible, only slightly shifted from the original position. This creation–annihilation process is repeated at most three times, finishing always when the magnetization precession of the gray domains crosses zero. For later times, the precession of m_y in the gray domains does not suffice to provoke the switching behavior, and the net magnetization along the vertical component of the core remains invariant.

The radically different behavior of the antivortex cores, compared to the vortex ones, can be understood either by the distinct trajectories of magnetic flux lines surrounding the two structures, or by the influence of the different dressing domain walls: the antivortex is located in the crossing point of four 90° DWs, whereas the vortices are surrounded by either three 90° plus two 45° DWs, or by two 90° plus four 45° DWs, depending on whether they are placed in the center or in the external sides of the microstructure, as in figure 4(b). In order to ascertain this, we show in panel (c) the corresponding images for one of the central vortex cores, in this case initially pointing down. It is evident that the core undergoes a very similar behavior of creation and annihilation of opposite m_z as for the previous vortex, again maintaining the original m_z core orientation, implying that the detailed surrounding of the vortex is irrelevant for its behavior.

We performed micromagnetic calculations with three different initial combinations of m_z at the vortex/antivortex cores, i.e. homogeneous [*uuuuuuu*], alternate [*udududu*], and random [*uddudud*], where *u* (*d*) denotes the core m_z pointing up (down), resulting in a statistical randomness of m_z switching at the vortex cores, independent of the vortex position in the microstructure. An example is shown in panel (d), where an initially-*d* vortex core reverses its m_z component. Strikingly, there are no significant differences in the images of panels (c) and (d) for $\Delta t = 150$ and 166 ps, although a clear *u* core appears at $\Delta t = 207$ ps, remaining while the initial vortex core is washed away. No core switching was ever observed in the case of antivortices, probably stabilized by the saddle point-like magnetic flux lines around them, which prevent the formation of opposite m_z circulating around. The described switching behavior of the vortex core agrees qualitatively with experimental [24] and calculated micromagnetic [8] studies of the vortex reversal, although they consider a squared and circular magnetic structure. From additional simulations on magnetic structures of squared and circular shapes, we can confirm the similar behavior of the vortex cores in the different environments. In this respect, the effect of additional DWs surrounding the vortex core is to dampen its overall dynamics. Although a better lateral resolution would be needed to clarify this, the random nature of the core switching for this range of exciting magnetic field strength is incompatible with the stroboscopic approach currently used, so that only single-shot measurements would be able to follow it.

4. Summary

In conclusion, we have demonstrated the temporal evolution of the different magnetic components present in a rectangular Py microstructured platelet under a triangular 80 Oe magnetic field pulse. A large magnetization precession is observed in the domains with initial magnetization perpendicular to

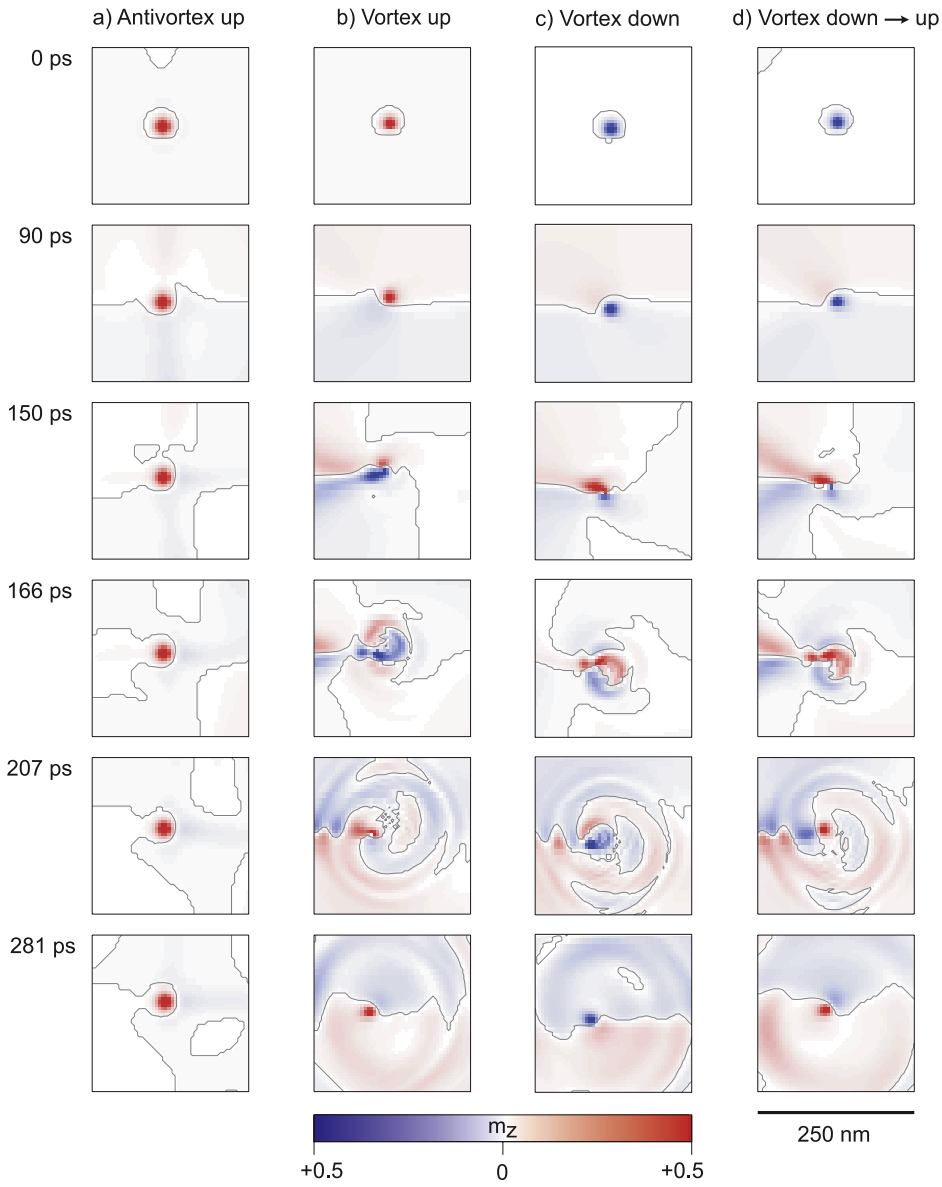

Figure 4. Zoomed-in plots of the calculated m_z components in the vicinity of one antivortex and several vortices at some selected delay times. For the sake of clarity, the color scale has been stretched so that values of m_z higher (lower) than $+0.5$ (-0.5) appear homogeneously red (blue). Contour lines for $m_z = 0$ are indicated as black lines.

the applied field, yielding a deviation of m_y of up to 20° with a frequency of 3.75 GHz. At longer timescales, the domain walls oscillate with a typical frequency of 1.25 GHz. The experimental XMCD-PEEM results are compared to micromagnetic calculations, yielding good agreement in time and frequency. We conclude from the calculations that only the vortex cores are susceptible to reverse their out-of-plane magnetization components, in a process triggered by the magnetization precession of the much larger gray domains and with random switching probability. In contrast, the antivortices seem to be insensitive to the magnetic pulse.

Acknowledgments

We gratefully acknowledge the Nano+Bio Center Kaiserslautern and F Radu for their help in the sample preparation; W Mahler and B Zada, in the measurements; M Fromme, for his computational assistance, and R Hertel, for the fruitful discussions on the calculations. This work was supported by the BMBF grant 05 KS4UK1/4.

References

[1] Back C H, Weller D, Heidmann J, Mauri D, Guarisco D, Garwin E L and Siegmann H C 1998 *Phys. Rev. Lett.* **81** 3251
[2] Choe S-B, Acremann Y, Scholl A, Bauer A, Doran A, Stöhr J and Padmore H A 2004 *Science* **304** 420
[3] Raabe J, Quitmann C, Back C H, Nolting F, Johnson S and Buehler C 2005 *Phys. Rev. Lett.* **94** 217204
[4] Lee K-S, Choi S and Kim S-K 2005 *Appl. Phys. Lett.* **87** 192502
[5] Buess M, Raabe J, Perzlmaier K, Back C H and Quitmann C 2006 *Phys. Rev.* B **74** 100404
[6] Lee K-S, Kim S-K, Yu Y-S, Choi Y-S, Guslienko K Y, Jung H and Fischer P 2008 *Phys. Rev. Lett.* **101** 267206

[7] Vansteenkiste A *et al* 2009 *Nature Phys.* **5** 332
[8] Hertel R, Gliga S, Fähnle M and Schneider C M 2007 *Phys. Rev. Lett.* **98** 117201
[9] Tretiakov O A and Tchernyshyov O 2007 *Phys. Rev.* B **75** 012408
[10] Komineas S 2007 *Phys. Rev. Lett.* **99** 117202
[11] Komineas S and Papanicolaou N 2008 *New J. Phys.* **10** 043021
[12] Guslienko K Y, Lee K-S and Kim S-K 2008 *Phys. Rev. Lett.* **100** 027203
[13] Choe S B, Acremann Y, Bauer A, Scholl A, Doran A, Stöhr J and Padmore H A 2004 *Synchrotron Radiat. Instrum.* **705** 1391
[14] Kuch W, Chelaru L I, Offi F, Kotsugi M and Kirschner J 2002 *J. Vac. Sci. Technol.* B **20** 2543
[15] Miguel J, Bernien M, Bayer D, Sánchez-Barriga J, Kronast F, Aeschlimann M, Dürr H A and Kuch W 2008 *Rev. Sci. Instrum.* **79** 033702
[16] http://math.nist.gov/oommf/
[17] Landau L D and Lifshiftz E M 1935 *Phys. Z. Sowjetunion* **8** 153
[18] Hubert A and Schäfer R 2000 *Magnetic Domains: the Analysis of Magnetic Microstructures* (Berlin: Springer)
[19] Neudert A, McCord J, Schäfer R, Kaltofen R, Mönch I, Vinzelberg H and Schultz L 2006 *J. Appl. Phys.* **99** 08F302
[20] Wiese N, McVitie S, Chapman J N, Capella-Kort A and Otto F 2007 *Europhys. Lett.* **80** 57003
[21] Park J P, Eames P, Engebretson D M, Berezovsky J and Crowell P A 2003 *Phys. Rev.* B **67** 020403
[22] Perzlmaier K, Buess M, Back C H, Demidov V E, Hillebrands B and Demokritov S O 2005 *Phys. Rev. Lett.* **94** 057202
[23] Kuepper K, Buess M, Raabe J, Quitmann C and Fassbender J 2007 *Phys. Rev. Lett.* **99** 167202
[24] Van Waeyenberge B *et al* 2006 *Nature* **444** 461